Project report 2
November 2018 - March 2019

Tungabhadra Left Bank Canal (TLBC) irrigation modernization: Detailed command area mapping using remote sensing

Murali Krishna Gumma, Kimeera Tummala, Mohammad Jameeruddin, Bhavani Pinjarla, P.S.Roy and Anthony M Whitbread

Submitted to
Advanced Centre for Integrated Water Resources Management (ACIWRM), WRD, Government of Karnataka

ICRISAT
INTERNATIONAL CROPS RESEARCH
INSTITUTE FOR THE SEMI-ARID TROPICS

Background:

Conventional surveys and assessments have merged with technology to help decision makers take timely action and prevent losses in agricultural production. Remote sensing is one such technology-driven tool that can produce accurate results economically. So is satellite imagery with high temporal and spatial resolutions specifically suited to agriculture. Given Karnataka state's diverse agro-ecosystems, knowing the spatial distribution of such systems and their constraints to production is essential so that abiotic stresses like drought can be mapped and information disseminated to decision makers for contingency planning.

The natural resource base of an area is instrumental in its agricultural development and also linked to improvement of livelihoods. Mapping the natural resource base and crop domains provides insights into the status of and trends in land and water utilization, development of water resources over time, and the impacts of cropping systems on water resource systems (Gumma et al. 2016a; Gumma et al. 2011a). Integrating remote sensing with spatial analyses like crop and economic models provides the much needed knowledge for decision making for resource-based planning of lower risk and profitable cropping systems, efficient allocation of water at basin and sub-basin levels and other crop management interventions in targeting technologies appropriate for different locations. Remote sensing provides such information in a time and cost effective manner by mapping major cropped areas using open datasets such as MODIS, LANDSAT, along with high resolution datasets from Indian remote sensing satellites, and sensors such as LISS IV and RiSAT-1 which provide reliable information on spatial distribution, acreage estimation and crop growth stages (during planting and harvesting).

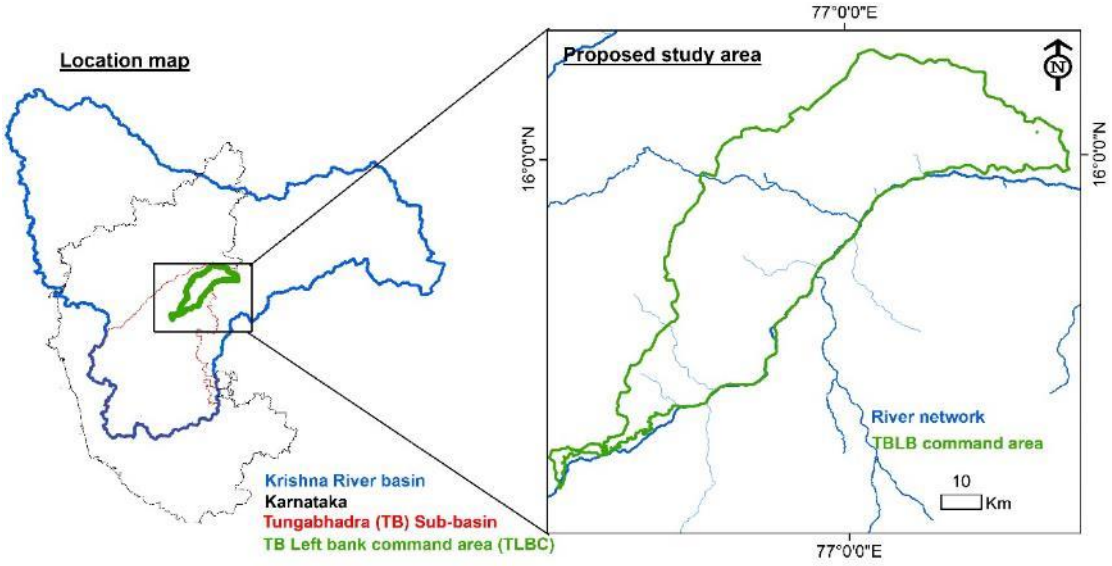

Figure 1. A map showing the study area.

Study area

The Krishna river basin is India's fourth largest covering 258,948 km^2 of southern India, spanning the states of Karnataka (113,291 km^2), Andhra Pradesh (31,638 km^2), Telangana (51,845 km^2) and Maharashtra (69,028 km^2) (Gumma et al. 2011c). The basin is relatively flat, except for the Western Ghats and some forested hills in the center and northeast. The river Krishna originates in the Western Ghat mountains, flows east across the Deccan Plateau, and discharges into the Bay of Bengal. It has three main tributaries that drain from the northwest, west and southwest (Figure 1). The climate is

generally semi-arid, with some dry, sub-humid areas in the eastern delta and humid areas in the Western Ghats. Annual precipitation averages 780 mm and decreases gradually from 850-1000 mm in the Krishna Delta to 300-400 mm in the northwest, then increases to >1000 mm in the Western Ghats. In the extreme western parts of the basin, the Western Ghats have high annual precipitation (1500-2500 mm). Most of the rainfall occurs during the monsoon from June to October. Cropping occurs in three seasons: Kharif during the monsoon (June to mid-December), rabi in the post-monsoon dry season (mid-December to March) and in the summer season (April and May). In Irrigated areas, rice during kharif season and other crops are grown in rabi season. Rainfed crops include cereals, pulses and oilseeds. The study will focus on Tungabhadra Left Bank Canal (TLBC) command area in Karnataka (nearly 250,000 ha).

Geographical area

Since the remote sensing-based intervention will mainly link to the hydrological analysis initiative of ACIWRM, Karnataka, the targeted intervention region is the Tungabhadra Left Bank Canal command area in Karnataka (Figure 1).

Component1

1.1. Ground data collection:

Ground truth data for kharif season was collected during 19-21 November 2018 in 113 sample sites covering major cropland areas (rainfed upland, lowland, irrigated, surface water, other non-agriculture land use) following the rainy season and with its fraction in a pixel of 90 m x 90 m at the location (Figure 1a). Observations were recorded extensively for class identification. In addition, a total of 455 observations were used for accuracy assessment. A minimum sampling unit of 90 m x 90 m was taken for ground truth validation at each location. At each sample site, information was collected on the existing crop, irrigation and soil types and land use land cover (LULC). The precise locations of the samples were recorded by a handheld Garmin GPS unit in tracking mode to map the total route travelled. The sample size varied from 15 to 20 for each category. At each location, a few photographs were taken to illustrate LULC during classification (Figures 1b and 1c). These data were collected based on stratified random sampling: stratified by road network and randomized by distance travelled (either every 10 minutes of drive or every 10/15/ 20 km, depending on road, weather conditions or other limitations like safety issues or sensitive locations). Roughly, 20% of all ground data samples were used for ideal spectra generation and class identification. Greater time was spent on ideal spectral sample locations since it took time to find local expert to speak to and to understand agricultural systems.

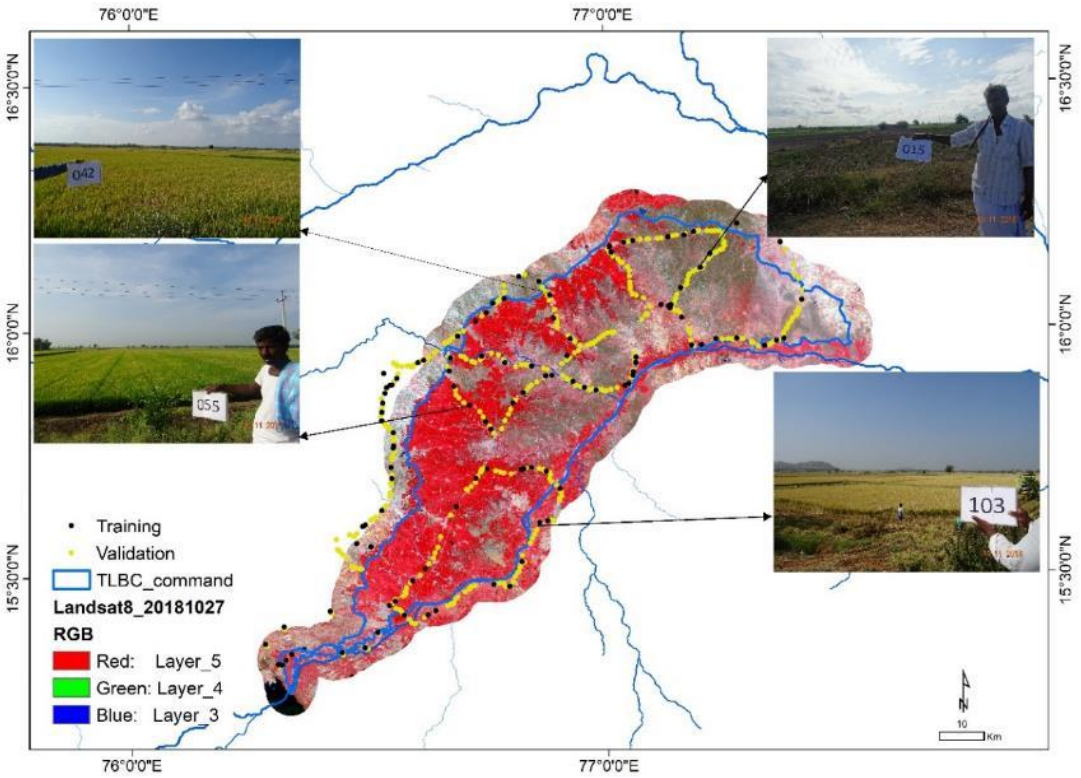

Figure 1*a:* Ground data collection – Kharif season 2018.

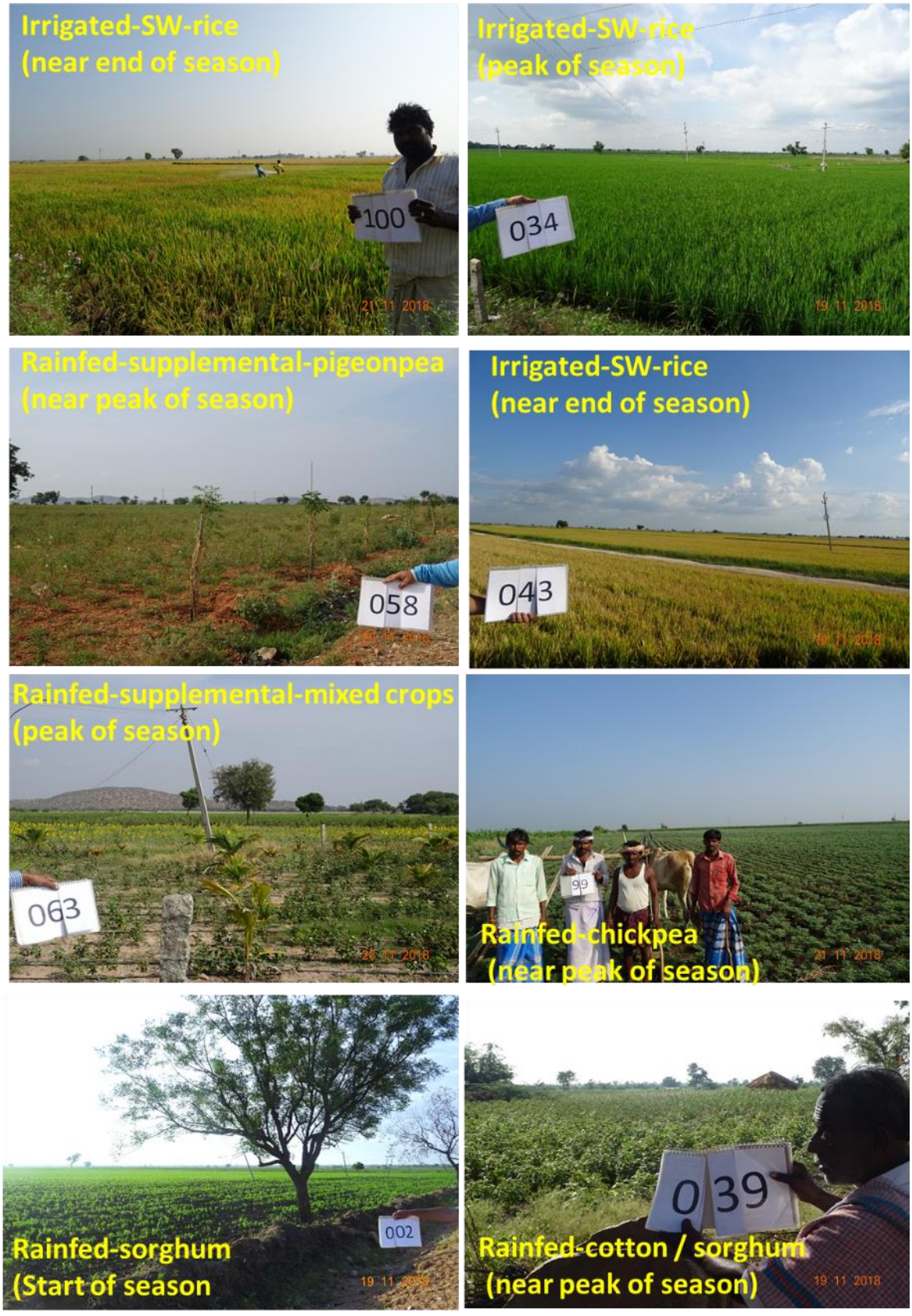

Figure 1b: Photographs of ground data with the crops and farmer interviews.

Figure 1c: Photographs of ground data with the crops and farmer interviews.

Ground truth data was similarly collected for rabi season from 15 - 19 February 2019, covering 105 sample sites of major cropland areas (rainfed upland, lowland, irrigated, surface water, other non-

agriculture land use) following the rainy season and with its fraction in a pixel of 90 m x 90 m at the location (Figure 2a). The ground truth collection scheme for rabi season is similar to that of the kharif season. Photographs taken at sample sites are shown in Figure 2b.

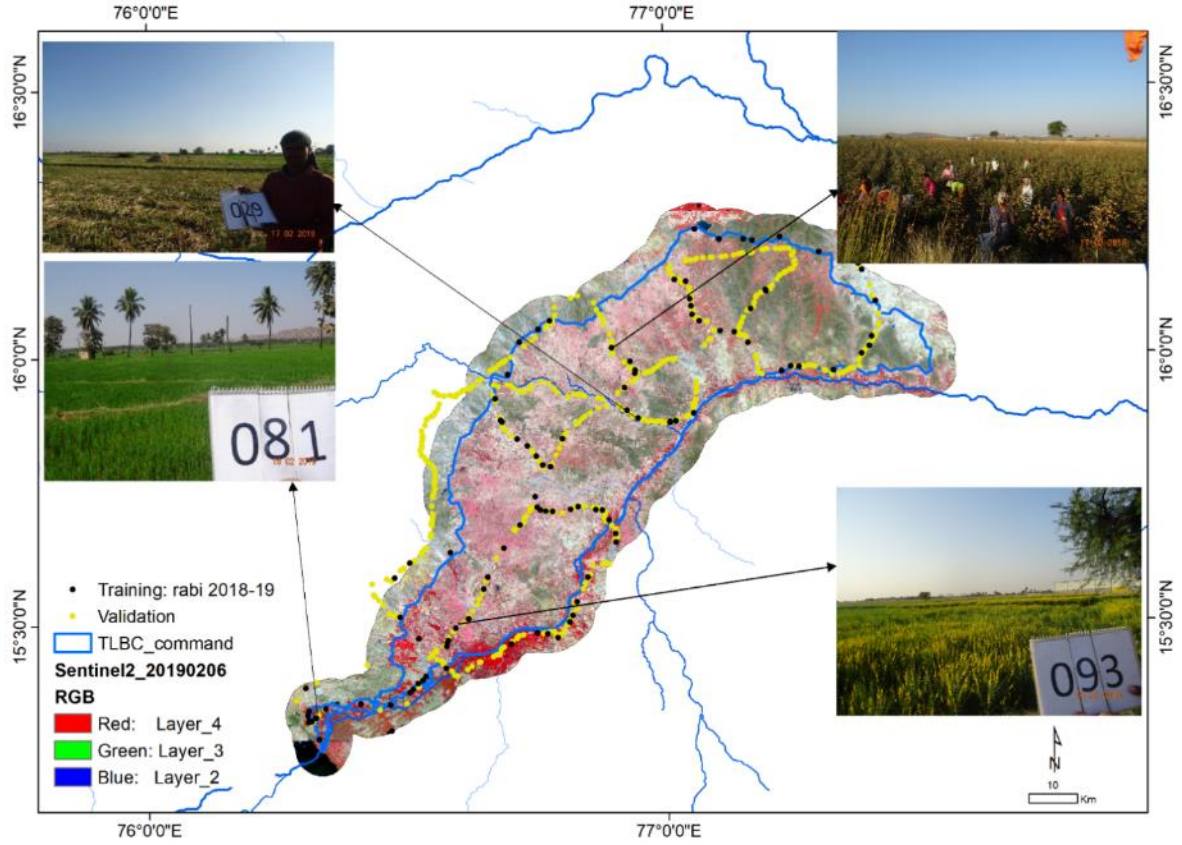

Figure 2*a:* Ground data collection – Rabi season 2018-19

Figure 2b: Photographs of ground data with the crops and farmer interviews.

Information on the irrigated area surrounding the point was categorized into three classes: small (≤10 ha), medium (10-15 ha), and large (≥15 ha). Additional information was gathered through interviews with farmers and district agriculture extension officers to determine crop intensity, and type during the previous year. Ground data was systematically collected by adopting the following approach:

- Cropland water methods: irrigated or rainfed
- Cropping intensity: single crop (SC), double crop (DC) or continuous crop (CC)
- Phenology: kharif or season 1 (June-October), rabi or season 2 (November-February).

Samples covered major cropland areas, which in turn were chosen based on the knowledge of the district agricultural extension officer in order to ensure adequate samples of major crops as well as other LULC information, including two photographs from each location. In many sample locations, farmers provided information on planting dates, cropping intensity (single or double crop), and percentage canopy cover for these locations. For areas not accessible due to road conditions and time constraints, additional information was obtained from agriculture and irrigation departments. LULC names and class labels were assigned in the field using the ground data protocol (Gumma et al. 2014; Thenkabail et al. 2009).

1.2. Crop dominance map @ 10 m

The process began with mapping land use/land cover using Sentinel-2 time series data with spectral matching techniques and ground data.

Six bands of Sentinel-2 data at 10 m resolution were obtained for September to December 2018. For each month, images with minimum cloud cover were used. Sentinel-2 datasets are available in the public domain and are pre-calibrated (https://earthexplorer.usgs.gov/). The large swath width of 290 km and a revisit time of 2-3 days at mid-latitudes because of the two-satellite constellation of Sentinel-2 makes it attractive for mapping large crop areas. The list of Sentinel-2 bands used in the present study is given in table 1. A total of 24 bands (6 bands from each of the Sentinel-2 images of the four months) were stacked and used for classification.

Table 1: Sentinel-2 bands used for classification, and their spatial resolutions.

Band	Resolution (m)
Band 2 - Blue	10
Band 3 - Green	10
Band 4 - Red	10
Band 8 - NIR	10
Band 11 - SWIR 1	20
Band 12 - SWIR 2	20

Unsupervised classification was used to generate initial classes. The unsupervised ISOCLASS cluster algorithm (ISODATA in ERDAS Imagine 2016TM) run on the 24-band stack generated an initial 60 classes, with a maximum of 60 iterations and convergence threshold of 0.99. Though ground survey data was available at the time of image classification, unsupervised classification was used in order to

capture the complete effect of all wavelengths over a large area. Use of unsupervised techniques is recommended for large areas that cover a wide and unknown range of vegetation types, and where landscape heterogeneity complicates identification of homogeneous training sites. Identification of training sites is particularly problematic for small, heterogeneous irrigated areas.

Land use/land cover classes were identified based on temporal signatures along with ground survey data. We observed crop growth stages including length of growing periods (LGPs) and cropping pattern from temporal signatures, such as (a) onset of cropping season (e.g., monsoon and winter); (b) duration of cropping season such as monsoon and winter; (c) magnitude of crops during different seasons and years (e.g., water stress and normal years); and (d) end of cropping season.

The process of labeling class identification was done based on spectral matching techniques (SMTs) (Gumma et al. 2018; Gumma et al. 2016b; Gumma et al. 2015). Initially, 160 classes from the unsupervised classification were grouped based on spectral similarity or closeness of class signatures. Each group of classes was matched with ideal spectral signatures and ground survey data, and assigned class names[1]. Classes with similar time series and land cover were merged into a single class, and classes showing significant mixing, e.g., homogeneous irrigated areas and forest, were masked and reclassified using the same ISOCLASS algorithm. Some continuous irrigated areas mixed with forests in the Western Ghats were separated using a 90 m digital elevation model (Papademetriou) from the Shuttle Radar Topography Mission (SRTM) and an elevation threshold of 630 m, Landsat imagery and ground survey data through spatial modeling techniques such as overlay, matrix, recode and proximity analysis. This resulted in 14 classes of LULC. While class aggregation could have been performed statistically using a Euclidean or other distance measure, we employed a user-intensive method that incorporates both ground survey data and high resolution imagery in order to avoid lumping classes that might be spectrally similar but have distinct land cover. The signatures of some classes differed in only one or two months, which would have caused the classes to be merged if an automated similarity index were used.

1.3. Accuracy assessment

Ground data points were used to assess the accuracy of the classification results, based on a standard procedure (Congalton and Green 1999; Congalton and Green 2008; Jensen 1996), to generate an error matrix and accuracy measures for each land use/land cover map. Error matrices and Equation (Farr and M. Kobrick) 'Cohen's kappa coefficient (κ)' are commonly used for accuracy assessment. For example, these are useful when building models that predict discrete classes or when classifying imagery. κ can be used as a measure of agreement between model predictions and reality (Congalton 1991) or to determine if the values contained in an error matrix represent a result significantly better than random (Jensen 1996). κ is computed as:

$$\kappa = \frac{N \sum_{i=1}^{r} x_{ii} - \sum_{i=1}^{r} (x_{i+} \times x_{+i})}{N^2 - \sum_{i=1}^{r} (x_{i+} \times x_{+i})} \quad (1)$$

where, N is the total number of sites in the matrix, *r* is the number of rows in the matrix*, xii* is the number in row *i* and column *i*, *x+i* is the total for row *i*, and *xi+* is the total for column *i* (Jensen 1996). The accuracy assessment for the classified map of kharif season consisting of 14 classes (both crop and other land use/ land cover classes) including overall accuracy, producer's and user's accuracies,

and kappa coefficient is given in Table 2a. Table 2b gives the corresponding crop dominance or land use/ land cover classes for the class names in Table 2a.

Table 2a: Accuracy assessment for the classified map of kharif season containing crop dominance along with other land use/land cover classes.

Classified Data	CL_1	CL_2	CL_3	CL_4	CL_5	CL_6	CL_7	CL_8	CL_9	CL_10	CL_11	CL_12	CL_13	CL_14	Classified totals	Number correct	Producers accuracy	User accuracy	Kappa
CL_1	95	0	0	0	0	0	0	0	0	0	0	0	0	0	95	95	86%	###	1.0
CL_2	10	21	0	0	0	0	0	0	0	0	0	0	0	0	31	21	100%	68%	0.7
CL_3	0	0	13	0	6	0	0	2	0	0	0	0	0	0	21	13	81%	62%	0.6
CL_4	0	0	1	13	1	0	0	1	0	0	0	1	0	0	17	13	37%	76%	0.7
CL_5	0	0	1	4	31	0	0	0	0	1	0	0	0	0	37	31	63%	84%	0.8
CL_6	0	0	0	0	0	0	0	0	0	0	0	0	0	0	0	0	--	---	0.0
CL_7	0	0	0	0	0	0	0	0	0	0	0	0	0	0	0	0	--	---	0.0
CL_8	1	0	1	0	0	0	0	30	0	0	1	1	0	0	34	30	81%	88%	0.9
CL_9	0	0	0	5	0	0	0	0	6	0	0	0	0	0	12	6	100%	50%	0.5
CL_10	0	0	0	0	0	0	0	0	0	0	0	0	0	0	0	0	--	---	0.0
CL_11	0	0	0	0	0	0	0	0	0	0	0	0	0	0	0	0	--	---	0.0
CL_12	1	0	0	10	9	1	0	3	0	2	1	3	0	0	30	3	60%	10%	0.1
CL_13	0	0	0	0	0	0	0	0	0	0	0	0	0	0	0	0	--	---	0.0
CL_14	3	0	0	3	2	1	0	1	0	0	0	0	0	0	10	0	--	---	0.0
Column Total	110	21	16	35	49	2	0	37	6	3	2	5	0	0	455	380			

Overall Classification Accuracy = 83.52%

Overall Kappa Statistics = 0.7910

Table 2b: Corresponding crop dominance and land use/ land cover classes for the class names in Table 2a.

Class name	Land use/ land cover
CL_1	01. Irrigated-SW-rice
CL_2	02. Irrigated-supplemental-rice
CL_3	03. Chickpea (CP)
CL_4	04. Irrigated-supplemental-cotton
CL_5	05. Sorghum
CL_6	06. Irrigated-supplemental-pigeonpea (PP) (Smith et al.)
CL_7	07. Irrigated-banana / sugarcane
CL_8	08. Mixed crops-sorghum-CP-cotton
CL_9	09. Mixed crops-CP-PP-sorghum
CL_10	10. Irrigated-supplemental-cotton/mixed crops

Class name	Land use/ land cover
CL_11	11. Fallows/CP/sorghum
CL_12	12. Shrub-lands/wastelands/gGrasses
CL_13	13. Water
CL_14	14. Built-up lands

The accuracy assessment for the classified map of rabi season consisting of 12 classes (both crop and other land use/ land cover classes) including overall accuracy, producer's and user's accuracies, and kappa coefficient is given in Table 3.

Table 3: Accuracy assessment for the classified map of rabi season containing crop dominance along with other land use/land cover classes.

	Validation data															
Classified data	CL_1	CL_2	CL_3	CL_4	CL_5	CL_6	CL_7	CL_8	CL_9	CL_10	CL_11	CL_12	Classified totals	Number correct	User's accuracy	Producer's accuracy
01. GW-rice	25	2	0	0	0	0	0	0	0	0	0	0	27	25	93%	86%
02.SW/GW-rice	0	33	0	0	0	1	0	3	0	0	0	1	38	33	87%	85%
03. Maize	0	0	8	0	0	0	0	0	0	0	0	0	8	8	100%	89%
04. Mustard	0	3	0	5	0	0	0	0	0	0	0	0	8	5	63%	71%
05. Chickpea	0	0	1	0	1	0	0	0	0	0	0	0	2	1	50%	100%
06. Banana/plantations	0	1	0	2	0	2	1	0	0	0	0	0	6	2	33%	67%
07. Sorghum	4	0	0	0	0	0	2	0	0	0	0	1	7	2	29%	50%
08. Cotton/fallows	0	0	0	0	0	0	0	9	0	0	0	0	9	9	100%	60%
09. Fallow	0	0	0	0	0	0	1	3	24	0	0	0	28	24	86%	100%
10. Mixed crops	0	0	0	0	0	0	0	0	0	4	0	0	4	4	100%	100%
11. Fallows/shrublands	0	0	0	0	0	0	0	0	0	0	2	0	2	2	100%	100%
12. Shrub lands/grasses	0	0	0	0	0	0	0	0	0	0	0	6	6	6	100%	75%
Total	29	39	9	7	1	3	4	15	24	4	2	8	145	121		

Overall accuracy = 83.45%
Kappa coefficient = 80.35%

1.4. Results

Spatial distribution of crops

Considering the objectives of this study and based on the methods described above and its sub-sections, distinct cropland classes of the study districts were mapped. The kharif season classified map for the TLBC command area is shown in Figure 3. The characteristics of these cropland classes were then used to determine croplands during the kharif season.

Table 4. Land use / land cover areas of the TLBC area with a 5 km buffer.

Land use / land cover	Area (ha)
01. Irrigated-SW-rice	173,187
02. Irrigated-supplemental-rice	35,074
03. Chickpea (CP)	21,625
04. Irrigated-supplemental-cotton	7,879
05. Sorghum	53,262

Land use / land cover	Area (ha)
06. Irrigated-supplemental-pigeonpea (Smith et al.)	704
07. Irrigated-banana / sugarcane	4,069
08. Mixed crops-sorghum-CP-cotton	100,222
09. Mixed crops-CP-PP-sorghum	27,659
10. Irrigated-supplemental-cotton/mixed crops	856
11. Fallows/CP/sorghum	13,350
12. Shrublands/wastelands/grasses	121,442
13. Water	11,145
14. Built-up lands	26,825
Total area	597,298
Total irrigated area	349,651

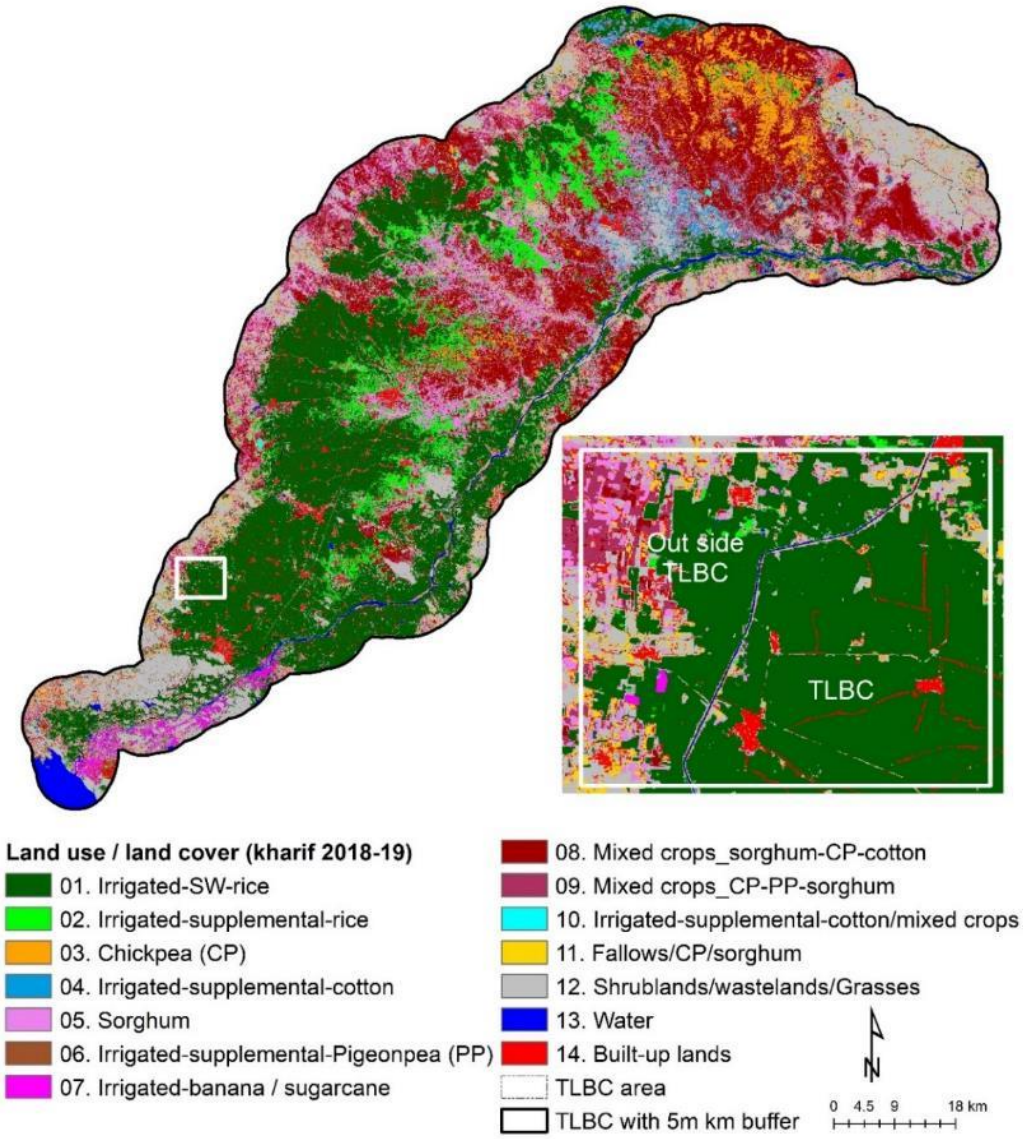

Figure 3: Classified map of the TLBC command area showing the spatial extent of dominant crops during kharif season along with other land use/ land cover classes.

The areas under various classes of the classified map for kharif season excluding the 5 km buffer are shown in table 5. Of the total cultivated area of 313,353 ha, the area under irrigation was found to be around 257,126 ha. The classified image without the 5 km buffer is shown in Figure 4.

Table 5. Land use / land cover areas of TLBC area without 5 km buffer.

Land use / land cover areas of TLBC areas	
Land use / land cover (kharif)	**Area (ha)**
01. Irrigated-SW-rice	128,304
02. Irrigated-supplemental-rice	31,052
03. Chickpea (CP)	17,154
04. Irrigated-supplemental-cotton	6,537
05. Sorghum	35,047
06. Irrigated-supplemental-pigeonpea (PP)	46
07. Irrigated-banana / sugarcane	93
08. Mixed crops-sorghum-CP-cotton	76,355
09. Mixed crops-CP-PP-sorghum	14,545
10. Irrigated-supplemental-cotton/mixed crops	193
11. Fallows/CP/sorghum	4,027
12. Shrublands/wastelands/Grasses	51,361
13. Water	2,443
14. Built-up lands	17,125
Total area	384,282
Total irrigated area	257,126

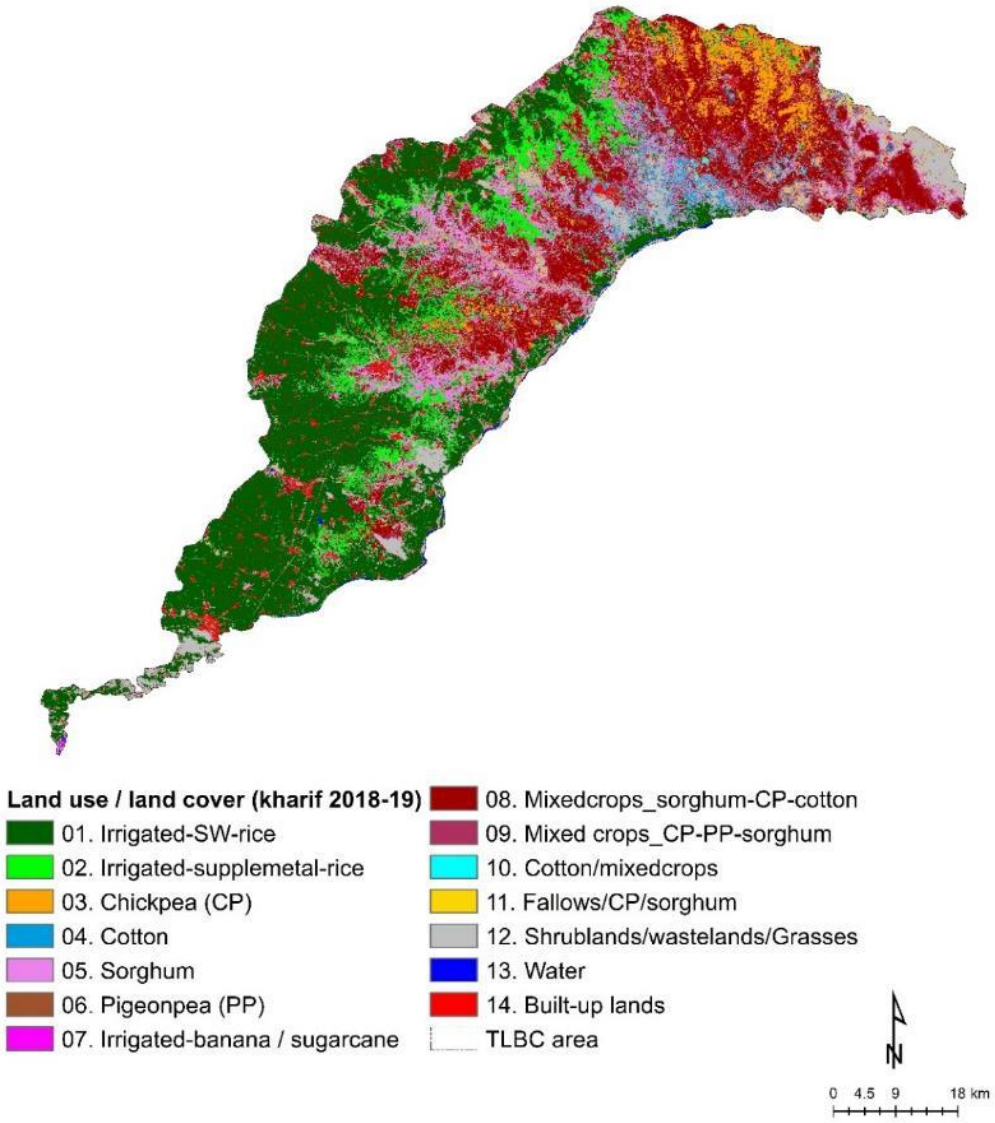

Figure 4: Classified map of the TLBC command area without the 5 km buffer, showing the spatial extent of dominant crops during kharif season along with other land use/ land cover classes.

For rabi season, the classified map with a 5 km buffer is shown in Figure 5, and the corresponding areas under various classes are shown in Table 6.

Table 6. Land use / land cover areas of TLBC areas with a 5 km buffer.

Land use / land cover (Roy et al.)	Area (ha)
01. GW-rice	2,711
02.SW/GW-rice	87,949
03. Maize	6,534
04. Mustard	13,047
05. Chickpea	6,585
06. Banana/plantations	9,457

Land use / land cover (Roy et al.)	Area (ha)
07. Sorghum	33,278
08. Cotton/fallows	27,326
09. Fallow	200,254
10. Mixed crops	16,698
11. Fallows/shrub lands	15,232
12. Shrub lands/grasses	138,896
13. Water bodies/wetlands	12,290
14. Built-up lands	26,838
Total area	597,095
Total irrigated area	100,117

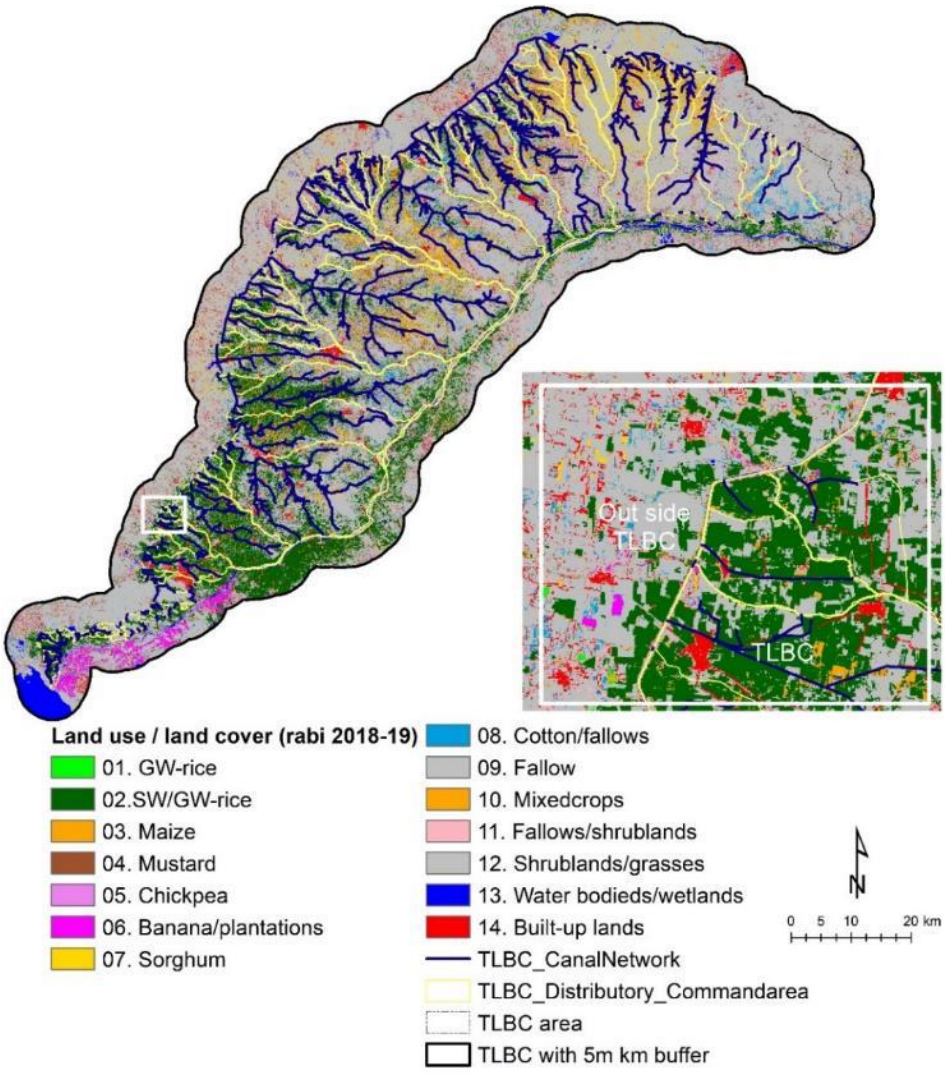

Figure 5: Classified map of the TLBC command area showing the spatial extent of dominant crops during rabi season along with other land use/ land cover classes.

The classified map of rabi season without the 5 km buffer is shown in Figure 6, and the corresponding areas are shown in Table 7. It was observed that the area under cultivation and thus the area under irrigation are both low in rabi season compared to kharif season. Out of the total cultivated area of 155,424 ha, 69,167 ha were irrigated in the rabi season.

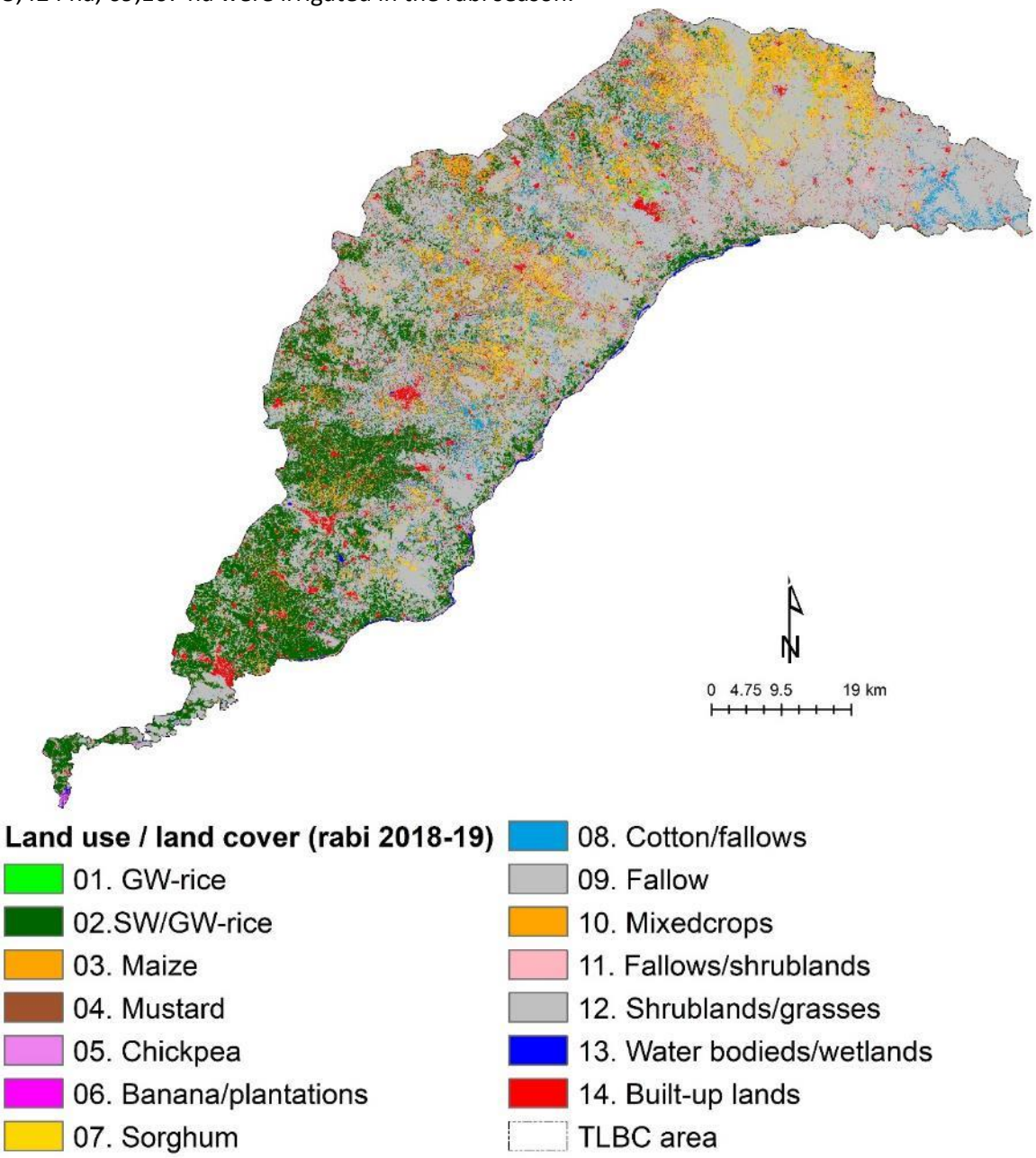

Figure 6: Classified map of the TLBC command area without the 5 km buffer showing the spatial extent of dominant crops during rabi season along with other land use/ land cover classes.

Table 7. Land use / land cover areas of TLBC areas without a 5 km buffer.

Land use / land cover (Roy et al.)	Area (ha)
01. GW-rice	2,075
02.SW/GW-rice	63,663
03. Maize	6,231
04. Mustard	12,332

Land use / land cover (Roy et al.)	Area (ha)
05. Chickpea	5,829
06. Banana/plantations	3,429
07. Sorghum	26,995
08. Cotton/fallows	21,018
09. Fallow	137,061
10. Mixedcrops	13,852
11. Fallows/shrublands	10,093
12. Shrublands/grasses	61,959
13. Water bodieds/wetlands	2,599
14. Built-up lands	17,146
Total area	384,282
Total irrigated area	69,167

End use

India is among countries that have created extensive areas under irrigation facilities. However, there is an increasing concern about some of the potential irrigation created not being brought into the functional system, low operating efficiency, less crop productivity, etc. System performance monitoring, evaluation and diagnostic analysis are key to appreciating improvements or inefficiencies in our irrigation projects. Irrigated lands' baseline inventory in spatial and time domains using spatial information technologies (satellite remote sensing, digital image processing, GIS and GPS) provides an array of performance evaluation matrices to address this issue. Regular monitoring will bridge the gap between the creation and utilisation of irrigation potential and for optimizing production and productivity from irrigated lands on a sustainable basis. The information thus generated can support on-farm developmental work like the construction of field channels and field drains, land levelling and shaping and introduction of conjunctive use of canal and tube well irrigation. The performance evaluation studies of irrigation projects build baseline inventory of irrigation infrastructure at large scale at desired time intervals.

The basic objective of an irrigation project is to improve the productivity of the land for agricultural produce with scientific application of water and other management inputs. Performance can therefore be judged, if we have answers to the following questions:

- Is the irrigation potential utilised vis-à-vis the potential created?
- Is the return on agricultural production and productivity achieved towards design crop yield (maximisation)?
- Is irrigation water being efficiently applied (managed)?
- Is there an improvement or deterioration in the irrigated lands development (due to salinity / alkalinity, waterlogging)?

To address these questions, 'time domain' and 'spatial domain' play important roles.

Time domain: The time span of performance evaluation can be (i) since the commissioning of the irrigation project, and or (Gumma et al.) in subsequent time periods.

Spatial domain: A canal irrigation project in India constitutes a hierarchical system of main canal, branch canals, distributaries, minors and field channels. Each has its irrigation command:

- A canal irrigation project in India is also divided and sub-divided into several administrative jurisdictions like Irrigation Zones / Divisions / Sub-divisions / Blocks.
- Each canal can be divided into 'head reach' and 'tail reach'.

Evaluation has to be structured into relative performance within the time domains and spatial domains of an irrigation project or among several irrigation projects.

Target audience and uses

1. Generation of spatial information on cropping pattern at command area level will help **stakeholders monitor the changes taking place between land uses like agricultural lands, fallows of different types (including major crops)** and land cover such as forest lands, water bodies and wetlands. Land use planning is possible with this type of information.
2. Crop dominance mapping is the primary task which will be useful in **acreage estimation** and **production monitoring**. **Administrators from the agricultural departments and revenue authorities will need such spatial information** at disaggregated administrative levels to disseminate advisories to farmers for timely inputs and crop protection practices.

Other outcomes and outputs include, but are not limited to:

- Improve the ability to monitor changes and implement effective land use planning across government agencies and people (planning, irrigation, agriculture, farmers, etc.)
- Timely dissemination of improved advisories to farmers related to inputs and crop protection practices
- Enhance productivity through better disseminated interventions
- Better farming practices related to improved seasonal rainfall and weekly rainfall predictions
- Stabilize prices in markets through improved regionally downscaled forecasts and subsequent yield and risk assessments to improve farmer decision making
- Improving agriculture productivity and water saving through new cropping pattern.

Future perspective

Traditional indicators of canal irrigation are equity, adequacy and reliability, and are estimated from the supply side. Equity assessment, however, reveals whether spatial and temporal water use across a canal command is consistent. Adequacy is the quantitative component, and is defined as the sufficiency of water use in an irrigation system. In contrast, reliability is the time component and defined as the correspondence of water supply upon request. These indicators of water supply to cropped area can be assessed using evaporative fraction maps (using satellite-derived evapotranspiration) which directly reveal crop supply conditions. However, in a canal command, where conjunctive water use is predominant, it is judicious to estimate them based on water consumed by crops.

Benchmarking of irrigation systems is a systematic process for securing continual improvement through comparison with relevant and achievable internal or external performance indicators. Attempts to assess performance or benchmark irrigation systems have often failed. One crucial reason

for this is the difficulty in identifying cost-effective performance monitoring indicators that can be assessed rapidly, consistently and continuously. Occasional assessment of irrigation system performance over vast areas has been greatly facilitated by high-resolution images acquired from satellites. They offer inexpensive, rapid and consistent methodologies to monitor spatial and temporal variation of large-scale processes. Over the past three decades, various combinations of images and algorithms have been used to estimate:

- Irrigated areas
- Cropping patterns
- Cropping intensity
- Soil moisture availability
- Evapotranspiration
- Crop water stress
- Land and water productivity
- Prospective yields and
- Extent of land degradation due to salinization, waterlogging, flooding and soil erosion.

Finally, it is also important to map areas under climate change "hot spots" by using climate information along with population density, agricultural land and gross domestic product (GDP) overlaid to identify 'hot spot' areas. Hot spot analysis could suggest the areas where more investments are needed to minimize irrigation risk and such investments are likely to have a substantial payoff in terms of reduced loss and sustainable agriculture.

References:

Congalton, R., & Green, K. (1999). Assessing the Accuracy of Remotely Sensed Data: Principles and Practices Lewis. *New York*

Congalton, R.G. (1991). Remote Sensing and Geographic Information System Data Integration: Error Sources and. *Photogrammetric Engineering & Remote Sensing, 57*, 677-687

Congalton, R.G., & Green, K. (2008). *Assessing the accuracy of remotely sensed data: principles and practices*. CRC press

Farr, T.G., & M. Kobrick (2000). Shuttle Radar Topography Mission produces a wealth of data,. *EOS Transactions, 81*, 583-585

Gumma, M.K., Charyulu Deevi, K., Mohammed, I.A., Varshney, R.K., Gaur, P., & Whitbread, A.M. (2016a). Satellite imagery and household survey for tracking chickpea adoption in Andhra Pradesh, India. *International Journal of Remote Sensing, 37*, 1955-1972

Gumma, M.K., Nelson, A., Thenkabail, P.S., & Singh, A.N. (2011a). Mapping rice areas of South Asia using MODIS multitemporal data. *Journal of Applied Remote Sensing, 5*, 053547-053547-053526

Gumma, M.K., Thenkabail, P.S., Deevi, K.C., Mohammed, I.A., Teluguntla, P., Oliphant, A., Xiong, J., Aye, T., & Whitbread, A.M. (2018). Mapping cropland fallow areas in myanmar to scale up sustainable intensification of pulse crops in the farming system. *GIScience & Remote Sensing, 55*, 926-949

Gumma, M.K., Thenkabail, P.S., Hideto, F., Nelson, A., Dheeravath, V., Busia, D., & Rala, A. (2011b). Mapping Irrigated Areas of Ghana Using Fusion of 30 m and 250 m Resolution Remote-Sensing Data. *Remote Sensing, 3*, 816-835

Gumma, M.K., Thenkabail, P.S., Maunahan, A., Islam, S., & Nelson, A. (2014). Mapping seasonal rice cropland extent and area in the high cropping intensity environment of Bangladesh using MODIS 500m data for the year 2010. *ISPRS Journal of Photogrammetry and Remote Sensing, 91*, 98-113

Gumma, M.K., Thenkabail, P.S., Muralikrishna, I.V., Velpuri, M.N., Gangadhararao, P.T., Dheeravath, V., Biradar, C.M., Acharya Nalan, S., & Gaur, A. (2011c). Changes in agricultural cropland areas between a water-surplus year and a water-deficit year impacting food security, determined using MODIS 250 m time-series data and spectral matching techniques, in the Krishna River basin (India). *International Journal of Remote Sensing, 32*, 3495-3520

Gumma, M.K., Thenkabail, P.S., Teluguntla, P., Rao, M.N., Mohammed, I.A., & Whitbread, A.M. (2016b). Mapping rice-fallow cropland areas for short-season grain legumes intensification in South Asia using MODIS 250 m time-series data. *International Journal of Digital Earth, 9*, 981-1003

Gumma, M.K., Uppala, D., Mohammed, I.A., Whitbread, A.M., & Mohammed, I.R. (2015). Mapping Direct Seeded Rice in Raichur District of Karnataka, India. *Photogrammetric Engineering & Remote Sensing, 81*, 873-880

Herold, M., Mayaux, P., Woodcock, C., Baccini, A., & Schmullius, C. (2008). Some challenges in global land cover mapping: An assessment of agreement and accuracy in existing 1 km datasets. *Remote sensing of environment, 112*, 2538-2556

Jensen, J.R. (1996). Introductory digital image processing: A remote sensing perspective. Upper Saddle River, New Jersey: Prentice Hall.

Papademetriou, M.K. (2000). Rice production in the Asia-Pacific region: Issues and perspectives. In M.K. Papademetriou, F.J. Dent, & E.M. Herath (Eds.), *Bridging the Rice Yield Gap in the Asia-Pacific Region* (p. 220). Bangkok Food and Agriculture Organization of the United Nations

Roy, P.S., Behera, M.D., Murthy, M.S.R., Roy, A., Singh, S., Kushwaha, S.P.S., Jha, C.S., Sudhakar, S., Joshi, P.K., Reddy, C.S., Gupta, S., Pujar, G., Dutt, C.B.S., Srivastava, V.K., Porwal, M.C., Tripathi, P., Singh, J.S., Chitale, V., Skidmore, A.K., Rajshekhar, G., Kushwaha, D., Karnatak, H., Saran, S., Giriraj, A., Padalia, H., Kale, M., Nandy, S., Jeganathan, C., Singh, C.P., Biradar, C.M., Pattanaik, C., Singh, D.K., Devagiri, G.M., Talukdar, G., Panigrahy, R.K., Singh, H., Sharma, J.R., Haridasan, K., Trivedi, S., Singh, K.P., Kannan, L., Daniel, M., Misra, M.K., Niphadkar, M., Nagabhatla, N., Prasad, N., Tripathi, O.P., Prasad, P.R.C., Dash, P., Qureshi, Q., Tripathi, S.K., Ramesh, B.R., Gowda, B., Tomar, S., Romshoo, S., Giriraj, S., Ravan, S.A., Behera, S.K., Paul, S., Das, A.K., Ranganath, B.K., Singh, T.P., Sahu, T.R., Shankar, U., Menon, A.R.R., Srivastava, G., Neeti, Sharma, S., Mohapatra, U.B., Peddi, A., Rashid, H., Salroo, I., Krishna, P.H., Hajra, P.K., Vergheese, A.O., Matin, S., Chaudhary, S.A., Ghosh, S., Lakshmi, U., Rawat, D., Ambastha, K., Malik, A.H., Devi, B.S.S., Gowda, B., Sharma, K.C., Mukharjee, P., Sharma, A., Davidar, P., Raju, R.R.V., Katewa, S.S., Kant, S., Raju, V.S., Uniyal, B.P., Debnath, B., Rout, D.K., Thapa, R., Joseph, S., Chhetri, P., & Ramachandran, R.M. (2015). New vegetation type map of India prepared using satellite remote sensing: Comparison with global vegetation maps and utilities. *International Journal of Applied Earth Observation and Geoinformation, 39*, 142-159

Smith, A., Snapp, S., Dimes, J., Gwenambira, C., & Chikowo, R. (2016). Doubled-up legume rotations improve soil fertility and maintain productivity under variable conditions in maize-based cropping systems in Malawi. *Agricultural Systems, 145*, 139-149

Thenkabail, P.S., Biradar, C.M., Noojipady, P., Dheeravath, V., Li, Y., Velpuri, M., Gumma, M., Gangalakunta, O.R.P., Turral, H., Cai, X., Vithanage, J., Schull, M.A., & Dutta, R. (2009). Global irrigated area map (GIAM), derived from remote sensing, for the end of the last millennium. *International journal of remote sensing, 30*, 3679-3733